NIH Public Access
Author Manuscript
Cancer Cell. Author manuscript; available in PMC 2013 January 17.

Published in final edited form as:
Cancer Cell. 2012 January 17; 21(1): 36–51. doi:10.1016/j.ccr.2011.12.004.

Bile acid and inflammation activate gastric cardia stem cells in a mouse model of Barrett's-like metaplasia

Michael Quante[1,8,*], **Govind Bhagat**[2], **Julian Abrams**[1], **Frederic Marache**[1], **Pamela Good**[1], **Michele D. Lee**[1], **Yoomi Lee**[1], **Richard Friedman**[3], **Samuel Asfaha**[1], **Zinaida Dubeykovskaya**[1], **Umar Mahmood**[4], **Jose-Luiz Figueiredo**[5], **Jan Kitajewski**[6], **Carrie Shawber**[6], **Charles Lightdale**[1], **Anil K. Rustgi**[7], and **Timothy C. Wang**[1,*]

[1]Division of Digestive and Liver Diseases, Irving Cancer Research Center, Department of Medicine, Columbia University Medical Center, New York, NY

[2]Department of Pathology and Cell Biology, Columbia University Medical Center, New York, NY

[3]Department of Biomedical Informatics, Columbia University Medical Center, New York, NY

[4]Nuclear Medicine & Molecular Imaging, Harvard Medical School and Massachusetts General Hospital, Boston, MA

[5]Center for Systems Biology, Harvard Medical School and Massachusetts General Hospital, Boston, MA

[6]Pathology, Obstetrics and Gynecology, and Herbert Irving Comprehensive Cancer Center, Columbia University Medical Center, New York, NY 10032, USA

[7]Division of Gastroenterology, Department of Medicine and Genetics, Abramson Cancer Center, University of Pennsylvania, Philadelphia, PA

[8]II. Medizinische Klinik, Klinikum rechts der Isar, Technische Universität München, Ismaninger Str. 22, 81675 München

Summary

Esophageal adenocarcinoma (EAC) arises from Barrett esophagus (BE), intestinal-like columnar metaplasia linked to reflux esophagitis. In a transgenic mouse model of BE, esophageal overexpression of interleukin-1β phenocopies human pathology with evolution of esophagitis, Barrett's-like metaplasia and EAC. Histopathology and gene signatures resembled closely human BE, with upregulation of TFF2, Bmp4, Cdx2, Notch1 and IL-6. The development of BE and EAC was accelerated by exposure to bile acids and/or nitrosamines, and inhibited by IL-6 deficiency. Lgr5+ gastric cardia stem cells present in BE were able to lineage trace the early BE lesion. Our data suggest that BE and EAC arise from gastric progenitors due to a tumor-promoting IL-1β-IL-6 signaling cascade and Dll1-dependent Notch signaling.

© 2011 Elsevier Inc. All rights reserved.

*Corresponding authors: Timothy C. Wang, M.D., Division of Digestive and Liver Diseases, Columbia University Medical Center, 1130 St. Nicholas Avenue, Room 925, 9th Floor; New York, NY 10032, Phone: (212) 851-4581; Fax: (212) 851-4590; tcw21@columbia.edu. Michael Quante, M.D., II. Medizinische Klinik, Klinikum rechts der Isar, Technische Universität München, Ismaninger Str. 22, 81675 München, Phone: +49 89 4140 6795; Fax: +49 89 4140 6796; Michael.Quante@lrz.tum.de.

Publisher's Disclaimer: This is a PDF file of an unedited manuscript that has been accepted for publication. As a service to our customers we are providing this early version of the manuscript. The manuscript will undergo copyediting, typesetting, and review of the resulting proof before it is published in its final citable form. Please note that during the production process errors may be discovered which could affect the content, and all legal disclaimers that apply to the journal pertain.

NIH-PA Author Manuscript
NIH-PA Author Manuscript
NIH-PA Author Manuscript

NIH-PA Author Manuscript

NIH-PA Author Manuscript

NIH-PA Author Manuscript

Introduction

Esophageal adenocarcinoma (EAC) has been linked to chronic inflammation of the esophagus and its incidence has increased by more than 500% since the 1970s (Corley et al., 2009) despite powerful acid suppressant medications (proton pump inhibitors) and a decline in the prevalence of *Helicobacter pylori* in the U.S and Europe. The main risk factor for EAC is Barrett Esophagus (BE), involving a progression from BE to low-grade/high-grade dysplasia (Falk, 2002). The precise origin of both EAC and BE has been difficult to discern in part because of the absence of useful experimental model systems that are genetically based.

BE has been attributed primarily to gastroesophageal reflux disease (GERD), leading to chronic inflammation of the esophagus. The link between inflammation and cancer is well established (Grivennikov et al., 2010); in particular, elevated IL-6 has been identified as a key mediator of tumorigenesis in murine models of cancer (Grivennikov and Karin, 2008). IL-1β, a pleiotropic pro-inflammatory cytokine upstream of IL-6 and TNF-α signalling cascades, has been demonstrated to induce tumorigenesis of the mouse stomach (Tu et al., 2008). IL-1β is overexpressed in BE, and clinical studies have suggested that polymorphisms in the *IL-1β* gene cluster are associated with BE (Fitzgerald et al., 2002; Gough et al., 2005; O'Riordan et al., 2005).

BE is defined as replacement of the stratified squamous epithelium in the distal esophagus with a metaplastic, intestinal-like columnar epithelium (Spechler et al., 2010). While attention in the past has been focused on goblet cells (i.e. classical intestinal metaplasia or IM) as the primary marker for BE, the recent change in the definition to include nongoblet, columnar lined esophagus (or CLE, resembling intestinal and cardia metaplasia) was made to acknowledge the more variable histologic presentation of BE. A major unanswered question that has been debated for decades, is whether the BE cell of origin derives from transdifferentiation of the esophageal squamous epithelium (Yu et al., 2005), or originates rather from a progenitor cell in the esophagus (Kalabis et al., 2008), the esophageal submucosal glands (Leedham et al., 2008), residual embryonic cells located at the squamocolumnar junction (Wang et al., 2011), or, as early investigators proposed, the gastric cardia (Allison and Johnstone, 1953; Barbera and Fitzgerald, 2010; Hamilton and Yardley, 1977; Nakanishi et al., 2007). However, prior to the development of IM, a regenerative intestinal-like columnar cell lineage appears in the esophagus that expresses TFF2, K8, K20, Notch and Cdx2 (Hanby et al., 1994; Menke et al., 2010; Stairs et al., 2008; Tatsuta et al., 2005). It is crucial to identify the progenitors responsible for BE, given the preneoplastic nature of the lesion.

Until recently, the primary animal model used to study BE has been a rat model comprising esophagojejunostomy that induces gastroduodenal reflux (Fein et al., 1998). The observation that duodenoesophageal reflux induces EAC in rats points to the importance of refluxed duodenal contents in the pathogenesis of BE. Bile acids, particularly unconjugated bile acids such as deoxycholate (DCA) that induce DNA damage, are one component of gastroduodenal reflux that have been linked strongly to the development of BE. Reflux injury in the esophagus results in chronic inflammation with upregulation of numerous cytokines, such as IL-1β, IL-6 and IL-8, that might contribute to the metaplastic and dysplastic conversion of BE (Fitzgerald et al., 2002). Here, we aimed to utilize a model of Barrett's-like metaplasia, involving overexpression of IL-1β, to provides insights into the origins of Barrett's esophagus.

NIH-PA Author Manuscript

NIH-PA Author Manuscript

NIH-PA Author Manuscript

Results

Interleukin-1β overexpression in the mouse esophagus induces esophagitis, Barrett's-like metaplasia, and neoplasia

To understand the pathogenesis of BE and EAC we generated a model of chronic esophageal inflammation, inserting the modified human *IL-1β* cDNA (Bjorkdahl et al., 1999) downstream of an Epstein-Barr virus (ED-L2) promoter that targets the oral cavity, esophagus, and squamous forestomach (Figure S1a) (Nakagawa et al., 1997). In two founder lines we observed high (Line 1) and low levels (Line 2) of specific esophageal (and forestomach) hIL-1β mRNA and protein expression (Figure 1a, b) that correlated with upregulated IL1-receptor-antagonist (IL1ra), indicative of IL-1 receptor signaling (Figure 1c). No hIL-1β mRNA and protein expression was observed in the glandular stomach or elsewhere (Figure 1a, d). *L2-IL-1β* mice developed splenomegaly (Figure S1c) that correlated with age dependent IL-1β expression levels (Figure 1b), consistent with a systemic inflammatory reaction and at least 10-fold elevated ($p<0.05$) circulating levels of IL-1β, TNFα (Figure S1d), and IL-6 (Figure 1d).

The esophagus and squamous forestomach in the low and high expressing *L2-IL-1β* mice were markedly thickened with a mixed acute and chronic inflammatory infiltrate compared to age-matched WT mice (Figure S1b). However, the major histopathological changes in *L2-IL-1β* mice occurred at the squamocolumnar junction (SCJ), an anatomical location where the squamous and gastric columnar epithelium meet (Figure 1e) and where the esophagus enters the stomach. Compared to the human SCJ, the mouse esophagus enters the stomach at the midpoint of the lesser curvature of the stomach, at the junction between the glandular stomach and squamous forestomach, forming a SCJ that traverses the entire stomach and resembles the Z-line in the human esophagus (Figure S1e). To determine whether the L2-IL-1β mice develop metaplasia resembling human BE, histological evaluation was performed on sagittal sections through the esophagus and stomach (yellow line Figure S1e). Based upon previously described criteria (Fox et al., 2000), a histopathological scoring system for the mouse SCJ was developed. In 100% (10/10) of the 6-month-old *L2-IL-1β* mice, we observed moderate inflammation and profound epithelial hyperplasia (Figure 1f) that was never observed in age-matched WT mice. Proliferation was increased significantly in the esophageal basal compartment (Figure 2a).

In *L2-IL-1β* mice that were 12–15 months of age, 90% (9/10) developed severe columnar metaplasia (Figure 1e, f) with mucus producing (*Muc5ac*+, PAS+) cells (Figure 2a) at the SCJ, similar to human BE. While classical goblet cells were not observed in *L2-IL-1β* mice, the mucus producing columnar cell types observed were consistent with Barrett's-like metaplasia. *Tff2*, a marker for metaplasia in human BE (Van De Bovenkamp et al., 2003; Warson et al., 2002), and also a oxyntic progenitor cell marker in the gastric corpus (Quante et al., 2010), was not expressed in the WT esophagus but was upregulated above the SCJ of *L2-IL-1β* mice harboring metaplasia but not in dysplasia (Figure 2a). Electron microscopy studies revealed nearly identical ultrastructural features (columnar cell type, microvilli, granules, mucins) in human and mouse BE (Figure 2b). At 20–22 months of age, 20% (2/9) of *L2-IL-1β* mice developed high-grade dysplasia (HGD) or intramucosal EAC (Figure 1e-g). These lesions were grossly visible within the distal end of the esophagus (Figure 1g) and were associated with significant weight loss (28% +/−4%, $p<0.05$; data not shown). During this stepwise progression to cancer, we observed a gradual increase in αSMA+ stromal myofibroblasts (Figure 2a) and increasing stroma global hypomethylation (Figure S2) in BE and HGD compared, consistent with other models of inflammation-induced cancer (Jiang et al., 2008). While hypomethylation was prominent in the stroma, we could not exclude (and indeed suspect) gene specific hypermethylation in epithelial cells as described in humans (Sato and Meltzer, 2006).

NIH-PA Author Manuscript

NIH-PA Author Manuscript

NIH-PA Author Manuscript

Within the epithelial compartment, we observed stabilization of nuclear β-catenin (Figure 2c), a finding suggested in gene expression microarrays of WT and HGD tissue following laser capture microdissection (LCM) of metaplastic lesions in *L2-IL-1β* mice (Table S1). This microarray analysis confirmed an upregulation of *β-catenin*, *EVI1* and *RRas* in the tumors, consistent with activation of these pathways. Pathway analysis also revealed markedly increased phosphorylation of Akt and Erk in HGD samples (Figure 2D), compared to only a slight increase in BE-like metaplasia, especially after bile acid treatment, and absent expression in WT cardia tissue (Figure 2D). We also observed occasional loss of p16 and increased c-Myc expression or stabilization of p53 in the neoplastic epithelium (Figure 2c, d), thus demonstrating involvement in our mouse model of BE/EAC of a number of pathways relevant to human BE and EAC.

Bile acids and carcinogens accelerate the development of Barrett's-like metaplasia and dysplasia that can be diagnosed endoscopically in the mouse

BE and EAC have been attributed to acid reflux leading to chronic esophagitis. In our mouse model of chronic inflammation, Barrett's-like metaplasia and dysplasia appeared to be more dependent upon IL-1*β* overexpression than acid exposure, since both WT mice and *L2-IL-1β* mice were kept on acidified water (pH≤2.0) but pathological changes were evident only in the *EL2-IL-1β* mice. Unconjugated bile acids are another component of gastroduodenal reflux that has been linked to the development of BE. Consequently, we treated 2–3 months old *L2-IL-1β* mice (line 2) and WT littermates with an unconjugated bile acid (BA, 0.2% deoxycholate) in the drinking water (pH 7) and analyzed the mice at 6, 9, 12 and 15 months (Figure S3a). Due to issues of solubility, BA were administered in pH 7.0 water, thus eliminating the possibility of acid exposure.

Six-month old BA-treated *L2-IL-1β* mice showed severe esophagitis with inflammatory infiltrates, but only moderate changes were observed in BA-treated WT mice (Figure 3a, b). Sixty percent (6/10) of 9-month-old BA-treated *L2-IL-1β* mice showed metaplastic changes at the SCJ, with higher overall metaplasia scores compared to untreated *L2-IL-1β* mice (2.7 *vs.* 1.8 $p<0.05$) (Figure 3a, S3c), indicating a significant acceleration by BA of Barrett's-like metaplasia. Moreover, we observed more severe metaplasia and dysplasia in BA-treated *L2-IL-1β* mice compared to untreated *L2-IL-1β* mice at both 12 months (dysplasia score 2.1 *vs.* 1.0 $p<0.05$) and 15 months (dysplasia score 2.4 *vs.* 1.4 $p<0.01$) (Figure 3a, S3c). Forty percent (4/9) of 15 month-old BA-treated *L2-IL-1β* mice presented with macroscopically visible tumors in the distal esophagus (Figure 3b), and exhibited significant weight loss consistent with partially obstructive lesions. These data suggest that BA play a significant role in the pathogenesis of BE and dysplasia, although we did not use bile acids at pH 2.0 and cannot rule out that gastric acid might also have a role in esophageal carcinogenesis.

N-Nitrosamines are generated typically at the SCJ from reduction of salivary nitrite to nitric oxide in response to gastric juice (Winter et al., 2007) and might play a role in the pathogenesis of BE. N-Methyl-N-nitrosourea (MNU) is a known gastric carcinogen for mice (Tomita et al., 2010), but does not appear to promote transformation of the non-inflamed esophageal epithelium (Figure S3a, b). Mucosa that is chronically inflamed is thought to be more sensitive to the effects of luminal carcinogens (Winter et al., 2007). Thus, in comparison to BA+MNU treated WT mice (Figure S3b), we observed a significant increase in tumor development in 12 month-old BA + MNU treated *L2-IL-1β* mice (Figure 3a, b).

Patients with EAC lose weight due to luminal obstruction, typically diagnosed by endoscopy and/or noninvasive imaging. Upper endoscopy in intact 15-month-old BA-treated or untreated *L2-IL-1β* (Movie S1-S2) and WT (Movie S3) mice after intubation and under constant ventilation (Figure 3c) revealed the luminal presence of BE-like metaplasia and tumor growth in the distal esophagus. The esophagi of *L2-IL-1β* mice showed

NIH-PA Author Manuscript

NIH-PA Author Manuscript

NIH-PA Author Manuscript

circumferential erythema and edema with inflammatory exudates compared to the normal esophagus (Figure 3c), changes that were increased in BA-treated *L2-IL-1β* mice. The endoscopic appearance resembled human BE (Movie S4). In 4 out of 9 BA-treated *L2-IL-1β* mice (15 month) but no *L2-IL-1β* mice (15 month), we observed obstructing tumors at the SCJ (Figure 3c and Movie S1-S3). 18F-FDG PET scans of BA-treated *L2-IL-1β* mice with endoscopically detected tumors revealed markedly increased focal glucose uptake, consistent with the severe inflammation in the esophagus and forestomach, along with tumorigenesis confirmed histologically (Figure 3d and Movie S5). These imaging data provide support for the acceleration of neoplastic processes in *L2-IL-1β* mice by BA.

Bile acids induce an acute and chronic immune response and activate differential gene expression in BE

Previous studies of IL-1β-induced carcinogenesis suggested that recruitment of myeloid cells is crucial for the development of neoplasia (Tu et al., 2008; Yang et al., 2010). In 6 month-old *L2-IL-1β* mice with mild esophagitis, there was no change in the abundance of CD4+ and CD8+ T cells or CD11b+/F4/80+ monocytes/macrophages in esophageal tissue, but a significant accumulation of immature (CD11b+Gr1+) myeloid cells (Figure 4c). At 9, 12, and 15-months, there was an even greater accumulation in *L2-IL-1β* mice of CD11b +Gr1+ cells in the esophagus (Figure 4c) and spleen (not shown) associated with chronic esophagitis and metaplasia. CD4+ T cells, F4/80+ macrophages and CD11b−Gr1+ neutrophils were also significantly increased but to a lesser extent in *L2-IL-1β* mice at these later time points (Figure 4b). Inflammatory cytokines were increased (Figure 1a–d and S1d) and the *L2-IL-1β* mice developed splenomegaly, likely due to an accumulation of immature splenic myeloid cells (Figure S1c). BA treatment resulted in additional increases in CD4+ T cells and CD11b−Gr1+ neutrophils, along with a slight decrease in CD11b+Gr1+ cells but no changes in CD11b+/F4/80+ macrophages (Figure 4a, b). These observations confirmed our histopathological scoring, showing more acute inflammation in BA-treated mice (Figure 3a). Our data suggest that BA may contribute to the development of BE by shifting the chronic inflammatory response towards an acute neutrophilic response. Recruited macrophages also suggest a role for tumor associated macrophages (TAMs) in BE.

In addition, 15-month BA-treated *L2-IL-1β* mice harboring metaplasia showed elevated levels of *Tff2*, *Cckbr*, *Muc5ac*, *Cdx2*, and *Krt19* (Figure 4d). *Bmp4*, *Cdx2*, and *Shh*, which are known to be involved in cellular differentiation and proliferation, were also associated with BA treatment (Figure 4d). Interestingly, we observed a significant upregulation of *Notch1* upon BA treatment, indicating a potentially important role for the Notch signaling pathway in BE and HGD (Figure 4D).

DLL1 dependent Notch signaling regulates differentiation and correlates with progression

Notch signaling is an essential factor in intestinal differentiation and seems to be required to maintain stem cells in an uncommitted state (Kim and Shivdasani, 2011). As with the intestinal epithelium, the Barrett's epithelium contains proliferative crypt-like compartments, and the Notch pathway has been found to be active in BE (Menke et al., 2010). Indeed, *Notch1* was upregulated significantly in the epithelium at the SCJ of BA-treated *L2-IL-1β* mice, compared to WT and untreated *L2-IL-1β* mice (Figure 4d, 5a, and S4a), pointing to a role of Notch signaling during EAC pathogenesis. Notch inhibition by systemic treatment with a γ-secretase inhibitor (DBZ), as reported previously (Menke et al., 2010), markedly increased both PAS+ cells and Alcian-Blue(+) goblet-like cells (Figure 5b, c), suggesting that inhibition of Notch signaling is associated with IM. Moreover, IHC for a general marker of activated Notch signaling (Notch intracellular domain or NICD, Figure S4a) revealed that NICD-expressing cells were predominantly found within columnar-lined esophagus (CLE) and dysplastic epithelial tissue at the SCJ, but not in IM at the SCJ, and

NIH-PA Author Manuscript

NIH-PA Author Manuscript

NIH-PA Author Manuscript

were in general not present in DBZ treated mice (Figure 5a and S4a) where we observed increased numbers of goblet cells (Figure 5c). These findings suggest that Notch signaling might contribute to the development of dysplasia, whereas inhibition of Notch signaling results in goblet cell differentiation and may prevent malignant transformation, although in theory both processes could occur simultaneously in different regions of the metaplastic epithelium.

We also observed upregulation of the Notch ligand Delta-like1 (*Dll1*) in BE-like tissue (Figure 5d and S4c, d), which correlated with increased Notch1 expression and proliferation in BE. Increasing numbers (Figure S4e) of *Dll1*-expressing cells could be found adjacent to Notch activated cells (Notch-IC), suggesting a possible intraepithelial crosstalk (Figure 5d). Most of the Dll1+ cells also expressed Tff2, supporting a concept of an expansion of Dll+ cells in the BE lineage (Figure S4f). In addition, we found downregulated Jagged2 gene expression in BE and EAC (Figure 6D, and Table S1) and were able to confirm decreased Jagged2 as assessed by IHC (Figure S4B), suggesting that Dll1, not Jagged2, is the predominant ligand inducing Notch signaling in BE. The location of Dlll1 expression was associated with the normal stem cell zone in the gastric cardia (data not shown), while Jagged2 appeared to be expressed in more terminally differentiated areas of the gastric cardia glands (Figure S4B, data not shown).

To confirm these findings from our mouse model, we analyzed 46 human BE biopsy samples. Biopsies were taken from Barrett's mucosa, evaluated by an expert gastrointestinal pathologist, and samples were classified histologically based on the highest degree of neoplasia present on any of the biopsies. *Notch1* was significantly upregulated in human biopsies of dysplastic tissues compared to BE tissue (Figure 5e), pointing to a role of Notch signaling in the development of EAC from BE. Overall, Notch activation appears to be associated with decreased goblet cell differentiation, as suggested by a lack of goblet cells in adjacent tissue of human EAC samples (unpublished data) and a review of the literature (Table S2). IHC for Notch intracellular domain (NICD) and Dll1 in human BE tissue showed a similar pattern, where expression of the receptor and ligand was found in adjacent but distinct cell types (Figure 5f).

Gene expression profiles of the IL-1β mouse esophagus closely resemble those of human Barrett's metaplasia and esophageal adenocarinoma

The gene expression profile of human BE (Stairs et al., 2008) is only slightly more similar to small intestine than it is to normal esophagus, in contrast to the striking similarity of BE morphology to intestinal morphology. Nevertheless, we found in both human BE and our mouse model that a number of gastric and intestinal genes were significantly upregulated. LCM was applied to typical metaplastic lesions in *L2-IL-1β* mice (with or without BA), and to the squamous epithelium of WT mice (Figure 6a). Compared to squamous epithelium, we observed 5698 genes with a significance cutoff of <0.05, that were differentially regulated in BE tissue of 15 month-old *L2-IL-1β* mice and 5950 genes in 9 months old BA-treated *L2-IL-1β* mice. Direct comparison of these two groups identified 1678 similarly upregulated (A in Venn diagram) and 2166 similarly downregulated (B in Venn diagram) genes (Figure 6b). In KEGG pathway analysis, these transcripts were enriched for cell adhesion molecules, adherens junctions, tight junctions, biosynthesis of unsaturated fatty acids, PPAR signaling pathway, and protein export. When compared to the earlier human expression analysis (GSE13083) (Stairs et al., 2008), entire sets of genes in the mouse were altered in the same directions (Figure 6c). KEGG pathway analysis of those genes that were identically up- or down-regulated in mouse and human, revealed changes in the expression of genes relevant for bile acid induced damage, signaling pathways (i.e. Notch), columnar cell related genes, and cell-cell contact genes (Figure 6d).

NIH-PA Author Manuscript

NIH-PA Author Manuscript

NIH-PA Author Manuscript

KEGG pathway analysis also identified genes that were altered differentially in BE-like epithelium of *L2-IL-1β* mice versus BA-treated *L2-IL-1β* mice (C-F in Venn diagram) with a significant overrepresentation of the biological processes of mismatch repair, adherens junction, apoptosis and autophagy, as well as alterations in signaling pathways with importance for carcinogenesis (Figure 6e). These results are consistent with a role for bile acids in promoting metaplasia and cancer by loosening cell-cell contacts, inducing oncogenic pathways, and causing cell death by DNA damage and oxidative stress.

Barrett's-like metaplasia and dysplasia correlate with expansion of gastric cardia progenitor cells in mice and humans

The current paradigm suggests that BE derives from de-differentiation or transdifferentiation of the squamous esophageal epithelium (Jankowski et al., 2000). To address the possible origins of BE in our mouse model, we examined the expression and localization of a number of putative stem cell or progenitor cell markers. Lgr5/GPR49 is a validated stem or progenitor cell marker for the mouse gut, but in the stomach it is expressed only in the gastric antrum and in the gastric cardia (Barker et al., 2010). Krt19 and Tff2 have been shown through lineage tracing studies to label different gastric progenitor cells (Means et al., 2008; Quante et al., 2010). Doublecortin and CaM kinase-like-1 (Dclk1), a microtubule-associated kinase expressed in neurons, has been postulated to be expressed in gut epithelial progenitors (Giannakis et al., 2006).

While the above markers were absent from the normal squamous esophageal epithelium, they showed increased expression over time in our *L2-IL-1β* mouse model, with expression first in the gastric cardia and later above the SCJ. In qRT-PCR studies Lgr5 was expressed minimally in the WT cardia, but could easily be detected in the cardia in 15 month old *L2-IL-1β* mice that showed features consistent with Barrett's metaplasia (Figure 7b). Lgr5 labeled cells were present in the cardia of Lgr5-Cre-ERTM mice crossed to Rosa-LacZ reporter mice shortly after tamoxifen induction, which within 7 days gave rise to lineage traced cardia epithelium in WT mice (Figure 7d), as previously shown (Barker et al., 2010). In *L2-IL-1β* mice crossed to Lgr5-Cre-ERTM/Rosa26-LacZ mice, we observed labeled BE metaplasia four month after tamoxifen induction followed by BA treatment at the age of 6–8 weeks (Figure 7d). These findings indicate that Lgr5+ cells within the cardia may function as progenitor cells, and thus potentially as the cells of origin for BE and dysplasia. Furthermore, we observed an increase in protein and mRNA expression of the *Krt19* gene (Figure 2a, 4d,), which is a known marker for surface mucus and gastric progenitor cells (Brembeck et al., 2001; Means et al., 2008), and. of the *Tff2* gene, expressed in gastric and cardia mucus neck and progenitor cells (Quante et al., 2010) and not in the normal esophageal epithelium (Figure 2a, 4d). Finally, we found an accumulation of Dclk1+ cells adjacent to the metaplastic mucus producing cells in BE tissue (Figure 7a, b). Dclk1+ cells are typically present as rare scattered cells localized primarily to the isthmus of the gastric glands (data not shown), but Dclk1+ cells are highly abundant in the gastric cardia, particularly just below the SCJ (Figure 7a). The gradual accumulation of Dclk1+ cells just above the SCJ in *L2-IL-1β* mice positively correlated with the development of metaplasia at the SCJ; with progression to dysplasia, Dckl1 expression was downregulated.

In human BE, qRT-PCR analysis showed a highly significant upregulation of *LGR5* and *DCLK1* compared to normal squamous epithelium (Figure 7c). Moreover, IHC for DCLK1 showed increased expression in dysplastic BE and decreased (or absent) expression of DCLK1 in dysplasia or adenocarcinoma (Figure 7a), similar to the observation in *L2-IL-1β* mice. Consistent with previous reports, TFF2 was highly expressed in Barrett's mucosa but not in biopsies of squamous esophageal epithelium (data not shown). Interestingly, LGR5 and DCLK1 were significantly elevated in the gastric cardia of BE patients (Figure 7e, f). The upregulation of gastric columnar progenitor cells in the region of the cardia and in BE

NIH-PA Author Manuscript

NIH-PA Author Manuscript

NIH-PA Author Manuscript

suggest that the metaplastic lineage in BE lesions in mice and humans may derive from a gastric cardia lineage (Figure 4g).

IL-6 deficiency abolishes inflammation, metaplasia and HGD in *L2-IL-1β* mice

IL-1β is upstream of IL-6 and TNF-α, which are both upregulated in our models (Figure S1d) and overexpression of IL-1β has been shown to induce tumorigenesis of the stomach (Tu et al., 2008). Persistent activation of the transcription factor signal transducer and activator of transcription-3 (Stat3) occurs in a large number of solid malignancies and supports the proliferation and survival of malignant cells, mostly triggered by an autocrine-paracrine production of IL-6 and family members (Bollrath et al., 2009). We observed elevated IL-6 protein levels in the serum and the SCJ of *L2-IL-1β* mice (Figure 1d), and IL-6 could be upregulated further by BA treatment (Figure 8a). IHC revealed increased pStat3+ cells during the progression from normal esophagus to BE and EAC (Figure 8b, c). Interestingly, we observed a significant upregulation of *IL-11Ra* and *Jak2*, and downregulation of *Socs3*, in our microarray analysis (Table S3). Given that we demonstrated increased levels of IL-6 and phosphorylated Stat3 in mouse BE-like and dysplasic tissues, *IL-11Ra* upregulation likely represents an inhibitory feedback mechanism. The finding of SOCS3 downregulation, as demonstrated recently (Watanabe et al., 2007), and increased levels of Jak2 with STAT3 activation, suggest a mechanism by which IL-1β and IL-6 could induce the development of cancer in our mouse model of BE/EAC.

In human EAC samples qRT-PCR analysis showed a significant upregulation of IL-6 and IL-1β compared to BE samples (Figure 8d, e), supporting our hypothesis that both cytokines play an important role during EAC pathogenesis. When we crossed *L2-IL-1β* mice with *IL-6*$^{-/-}$ mice we observed a complete abolishment of the metaplastic and dysplastic phenotype in homozygous *L2-IL-1β*/IL-6$^{-/-}$ mice, and a partly diminished phenotype with little metaplasia and no dysplasia in heterozygous *L2-IL-1β/IL-6*$^{-/+}$ mice (Figure 8f). In *L2-IL-1β/IL-6*$^{-/-}$ mice, we observed only a minor inflammatory response, which was increased in *L2-IL-1β/IL-6*$^{-/+}$ mice, but no increase in pSTAT3+ cells could be detected (data not shown). These data indicate that IL-1β mediates its carcinogenic effect in part through IL-6, suggesting the presence of a tumor-promoting IL-1β-IL-6-pStat3 signaling cascade in mouse EAC.

Discussion

Using a transgenic mouse model of esophageal inflammation, we demonstrate that increased IL-1β expression is sufficient for the induction of Barrett's-like metaplasia and dysplasia at the SCJ, extending previous findings in the glandular stomach (Tu et al., 2008) and affirming a crucial role for IL-1β in carcinogenesis, which is highly upregulated in human BE and EAC (Fitzgerald et al., 2002). Gene expression analysis, IHC, EM, and endoscopy provided evidence that our IL-1β mouse model closely resembles human disease, despite the fact that the mouse stomach differs from the human stomach. Inflammation in the squamous esophagus resulted in migration of cardia progenitor cells (including Lgr5+ cells) and their metaplastic descendants into the esophagus. We would conclude then that Barrett's esophagus is derived from gastric cardia progenitors at the SCJ junction.

While our L2-IL-1β mouse model exhibits a columnar-lined esophagus (CLE) but lacks abundant goblet cells (or classical IM), it is increasingly recognized that BE does not require classical IM to establish the diagnosis (Ogiya et al., 2008; Playford, 2006). Several studies have indicated that the risk of progression to EAC is the same in patients with CLE without goblet cells as it is in patients with IM (Gatenby et al., 2008; Goldblum, 2010; Kelty et al., 2007; Odze and Maley, 2010; Riddell and Odze, 2009; Takubo et al., 2009) (Table S2), and our clinical experience would support this broader premise. The findings that dysplasia tends

NIH-PA Author Manuscript

NIH-PA Author Manuscript

NIH-PA Author Manuscript

to recur following radiofrequency ablation in the presence of CLE without classical IM would support this model (Vaccaro et al., 2011). Notch inhibition has been associated with goblet cell differentiation (Menke et al., 2010), and thus the absence of Tff3+ or Muc2+ goblet cells may be related to the high levels of Notch expression. Our study adds to the evidence challenging the notion that metaplastic non-goblet cell CLE is entirely benign, and we would even argue that TFF2 has many advantages as a marker for BE, since it seems to be expressed early in the development of CLE, a lesion we postulate is the primary precursor lesion for EAC. Nevertheless, further studies in patients are needed to clarify the prognostic and diagnostic value of IM and CLE, since at present it remains controversial as to which metaplastic epithelial subtype best defines Barrett's Esophagus (Chatelain and Flejou, 2003), leading to controversial risk estimates for the development of HGD or EAC in BE patients (Hvid-Jensen et al., 2011).

IL-1β overexpression was able to induce metaplasia and dysplasia of the SCJ in part through recruitment of immature myeloid cells (IMC), which have been linked to carcinogenesis (Stairs et al., 2011; Tu et al., 2008; Yang et al., 2010). IMC were increased early in the distal esophagus and likely contribute to esophageal inflammation and carcinogenesis through secretion of pro-inflammatory cytokines (IL-6 and Tnf-α) and chemokines (Sdf1). With BA treatment, there was acceleration of dysplasia and a shift in the myeloid phenotype more towards granulocytic differentiation, pointing to the possible significance of a mixed acute/chronic inflammatory response in carcinogenesis (Fridlender et al., 2009). IL-6 levels were systemically elevated in *L2-IL-1β* mice, and the addition of IL-6 deficiency completely abrogated the IL-1β induced phenotype, indicating the importance of systemic immune activation in the development of neoplasia. Persistent activation of Stat3 through IL-6 additionally supports the proliferation and survival of malignant cells in mouse and human EAC, in contrast to the importance of IL-11 in carcinogenesis of the antrum (Ernst et al., 2008; Howlett et al., 2009). IL-6 in most tissues is a critical mediator of cancer initiation and progression, and IL-6-Stat3 inhibition may be a useful target for prevention or treatment of BE and EAC.

Unconjugated BA, which are increased in the refluxate of patients with BE (Kauer et al., 1997) and in patients on a high fat diet (Theisen et al., 2000), accelerated the development of BE and dysplasia. Unconjugated BA can induce gene promoter demethylation leading to activation of *IL-6*, *Cdx2* or *Notch1* gene expression in esophageal cells (Jankowski et al., 1999; Kazumori et al., 2006), a finding we can confirm in our BA- treated *L2-IL-1β mice*. Thus, through modulation of gene expression, unconjugated bile acids may promote an intestinal lineage commitment by progenitors. Pathway analysis of our gene expression studies confirm previously suggested carcinogenic roles for BA (Bernstein et al., 2005; Bernstein et al., 1999; Dvorak et al., 2007; Payne et al., 2005).

While it is generally accepted that BE and EAC arise from a common progenitor cell, the precise type and location of this cell remained unresolved. Temporal analysis of the *L2-IL-1β* mouse SCJ at different stages of the disease showed an initial expansion of progenitors in the gastric cardia, followed by migration over time into the esophagus (Figure 4g). LgR5 cell lineage tracing studies demonstrated the likely origin of at least some of the metaplastic BE tissue from Lgr5+ cells within the gastric cardia, where Lgr5+ cells also serve as functional cardia stem or progenitor cells. Furthermore, progenitor markers were essentially absent from the normal esophageal squamous epithelium, but Lgr5 (Barker et al., 2010), Tff2 (Quante et al., 2010), Krt19 (Means et al., 2008), Cck2r (Jin et al., 2009), and Dclk1 (Giannakis et al., 2006) were all present in the normal mouse gastric cardia, and were significantly increased in BE. Analysis of a cohort of human patients with BE showed a significant increase of identical progenitor markers in both gastric cardia and BE tissue.

NIH-PA Author Manuscript

NIH-PA Author Manuscript

NIH-PA Author Manuscript

However, our findings that Lgr5+ cardia cells can contribute to BE does not exclude contributions from other lineages. In addition, the use of mouse models to investigate the origins of human metaplasia has its limitations, given the anatomical differences. The predominant theory for the origins of Barrett's esophagus is based on the notion of reflux-induced transdifferentiation of squamous epithelial cells (Barbera and Fitzgerald, 2010; Yu et al., 2005). In addition, genetic evidence has supported the possible origin from multipotent progenitors present in submucosal squamous gland ducts, which are not present in the mouse and thus could not be examined in our model (Jankowski et al., 2000; Leedham et al., 2008). A recent study of *p63-null* mice led to the proposal that Barrett's-like metaplasia may arise from a population of Car4+/Krt7+ embryonic progenitors at the squamocolumnar junction (Wang et al., 2011). However, each of these alternative hypotheses, while reasonable, is also limited to date by the absence of dynamic lineage tracing and the sort of mechanistic underpinnings provided by our model.

Notch signaling appears important in the regulation of stem cell differentiation, and our data suggest that Dll1 is the major ligand inducing activated Notch signaling in BE, while Jagged2 may acts as an inhibitor, similar to a model of antagonism between different Notch ligands suggested previously (Benedito et al., 2009). In the cardia, DII1 was expressed at the bottom of the crypts adjacent to the location of LgR5 cells. Notch activation in Lgr5+ cells has been shown to correlate with lineage tracing at the SCJ at the cardia (Kim and Shivdasani, 2011), consistent with our hypothesis that Lgr5 cells from the gastric cardia migrate into the distal esophagus to give rise to BE tissue with increased Notch activation and Lgr5 expression. With the expansion of progenitor cells in BE, we observe a similar expansion of DII1+ cells immediately adjacent to Notch expressing cells within the metaplastic lineage. The strong correlation between DII1 with the progenitor cell zone and proliferation, and Jagged2 with post-mitotic, differentiated cells, suggests a potential mechanism for modulation of progenitor cell expansion and differentiation through Notch signaling. In this model, DII1 promotes progenitor cell maintenance and proliferation, and while Jagged2 inhibits proliferation and promotes differentiation, both a consequence of intraepithelial crosstalk between progenitor cells and their progeny. We would further hypothesize, that the development of IM occurs in a low Notch signaling environment, while maintenance of the CLE phenotype and progression to dysplasia occurs in a high Notch signaling environment.

Taken together, our data strongly suggest that BE arises from a gastric cardia lineage, as originally suggested (Hamilton and Yardley, 1977). Indeed, it has been difficult to distinguish at the histopathological level between so-called esophagogastric "junctional tumors" that appear localized to the cardia, and EAC, clearly present in the esophagus. The fact that BE always begins precisely at the SCJ has never otherwise been explained, and it now seems clear that special consideration should be given to "carditis", inflammation of the gastric cardia that may represent a precursor lesion of BE and EAC.

Experimental Procedures

For a detailed description of all methods see supplemental experimental procedures.

Mice

All mice studies and breeding were carried out under the approval of IACUC of Columbia University. Human *IL-1β* transgenic mice were generated by targeting expression of hIL-1β to the esophagus using the Epstein Bar virus promoter. Mice were placed on drinking water containing bile acids (0.3% DCA, pH 7.0) at the age of three months. Nine month-old L2-IL-1β mice were subjected to a 5-day treatment regimen with the GSI (DBZ, 30 mmol/kg). Lineage tracing studies were performed with Lgr5-CreTM-IRES-GFP mice crossed to

NIH-PA Author Manuscript

NIH-PA Author Manuscript

NIH-PA Author Manuscript

Rosa26R-LacZ reporter and L2-IL-1β mice. Tamoxifen (6mg) was given at the age of 6–8 weeks prior to administration of BA.

Human study

Esophageal tissue was obtained from 46 patients with BE, with and without dysplasia. Biopsies were taken for clinical and research purposes. This study was approved by the Columbia University Institutional Review Board and informed consent was obtained from all patients.

Accession number

Micro array information were deposited at the GEO database (http://www.ncbi.nlm.nih.gov/geo/) with the accession number GSE24931.

Supplementary Material

Refer to Web version on PubMed Central for supplementary material.

Acknowledgments

These studies are supported by NIH grants (RO1DK060758, 1U54CA126513, and R01CA120979) to T.C. Wang; NIH U01 grant (5U01 CA143056) to A.K. Rustgi, T.C. Wang and U. Mahmood. A.K. Rustgi was further supported by NIH P01-CA098101 and P30-DK050306 grants. M. Quante was supported by a grant from the Mildred-Scheel-Stiftung, Deutsche Krebshilfe, Germany. J. Abrams is supported by a Career development Award from the NCI (K07 CA132892) and by a Louis V. Gerstner, Jr. Scholars Award. We acknowledge the assistance of the Transgenic Mouse and Genomics Core of the Irving Cancer Research Center at Columbia University, and the Electronic Microscopy Core Facility at the University of Pennsylvania. We thank all members of the Wang lab for fruitful discussions.

References

Allison PR, Johnstone AS. The oesophagus lined with gastric mucous membrane. Thorax. 1953; 8:87–101. [PubMed: 13077502]

Barbera M, Fitzgerald RC. Cellular origin of Barrett's metaplasia and oesophageal stem cells. Biochem Soc Trans. 2010; 38:370–373. [PubMed: 20298185]

Barker N, Huch M, Kujala P, van de Wetering M, Snippert HJ, van Es JH, Sato T, Stange DE, Begthel H, van den Born M, et al. Lgr5(+ve) stem cells drive self-renewal in the stomach and build long-lived gastric units in vitro. Cell Stem Cell. 2010; 6:25–36. [PubMed: 20085740]

Benedito R, Roca C, Sorensen I, Adams S, Gossler A, Fruttiger M, Adams RH. The notch ligands Dll4 and Jagged1 have opposing effects on angiogenesis. Cell. 2009; 137:1124–1135. [PubMed: 19524514]

Bernstein H, Bernstein C, Payne CM, Dvorakova K, Garewal H. Bile acids as carcinogens in human gastrointestinal cancers. Mutat Res. 2005; 589:47–65. [PubMed: 15652226]

Bernstein H, Payne CM, Bernstein C, Schneider J, Beard SE, Crowley CL. Activation of the promoters of genes associated with DNA damage, oxidative stress, ER stress and protein malfolding by the bile salt, deoxycholate. Toxicol Lett. 1999; 108:37–46. [PubMed: 10472808]

Bjorkdahl O, Akerblad P, Gjorloff-Wingren A, Leanderson T, Dohlsten M. Lymphoid hyperplasia in transgenic mice over-expressing a secreted form of the human interleukin-1beta gene product. Immunology. 1999; 96:128–137. [PubMed: 10233687]

Bollrath J, Phesse TJ, von Burstin VA, Putoczki T, Bennecke M, Bateman T, Nebelsiek T, Lundgren-May T, Canli O, Schwitalla S, et al. gp130-mediated Stat3 activation in enterocytes regulates cell survival and cell-cycle progression during colitis-associated tumorigenesis. Cancer Cell. 2009; 15:91–102. [PubMed: 19185844]

Brembeck FH, Moffett J, Wang TC, Rustgi AK. The keratin 19 promoter is potent for cell-specific targeting of genes in transgenic mice. Gastroenterology. 2001; 120:1720–1728. [PubMed: 11375953]

NIH-PA Author Manuscript

NIH-PA Author Manuscript

NIH-PA Author Manuscript

Chatelain D, Flejou JF. High-grade dysplasia and superficial adenocarcinoma in Barrett's esophagus: histological mapping and expression of p53, p21 and Bcl-2 oncoproteins. Virchows Arch. 2003; 442:18–24. [PubMed: 12536310]

Corley DA, Kubo A, Levin TR, Block G, Habel L, Rumore G, Quesenberry C, Buffler P. Race, ethnicity, sex and temporal differences in Barrett's oesophagus diagnosis: a large community-based study, 1994–2006. Gut. 2009; 58:182–188. [PubMed: 18978173]

Dvorak K, Payne CM, Chavarria M, Ramsey L, Dvorakova B, Bernstein H, Holubec H, Sampliner RE, Guy N, Condon A, et al. Bile acids in combination with low pH induce oxidative stress and oxidative DNA damage: relevance to the pathogenesis of Barrett's oesophagus. Gut. 2007; 56:763–771. [PubMed: 17145738]

Ernst M, Najdovska M, Grail D, Lundgren-May T, Buchert M, Tye H, Matthews VB, Armes J, Bhathal PS, Hughes NR, et al. STAT3 and STAT1 mediate IL-11-dependent and inflammation-associated gastric tumorigenesis in gp130 receptor mutant mice. J Clin Invest. 2008; 118:1727–1738. [PubMed: 18431520]

Falk GW. Barrett's esophagus. Gastroenterology. 2002; 122:1569–1591. [PubMed: 12016424]

Fein M, Peters JH, Chandrasoma P, Ireland AP, Oberg S, Ritter MP, Bremner CG, Hagen JA, DeMeester TR. Duodenoesophageal reflux induces esophageal adenocarcinoma without exogenous carcinogen. J Gastrointest Surg. 1998; 2:260–268. [PubMed: 9841983]

Fitzgerald RC, Abdalla S, Onwuegbusi BA, Sirieix P, Saeed IT, Burnham WR, Farthing MJ. Inflammatory gradient in Barrett's oesophagus: implications for disease complications. Gut. 2002; 51:316–322. [PubMed: 12171950]

Fox JG, Beck P, Dangler CA, Whary MT, Wang TC, Shi HN, Nagler-Anderson C. Concurrent enteric helminth infection modulates inflammation and gastric immune responses and reduces helicobacter-induced gastric atrophy. Nat Med. 2000; 6:536–542. [PubMed: 10802709]

Fridlender ZG, Sun J, Kim S, Kapoor V, Cheng G, Ling L, Worthen GS, Albelda SM. Polarization of tumor-associated neutrophil phenotype by TGF-beta: "N1" versus "N2" TAN. Cancer Cell. 2009; 16:183–194. [PubMed: 19732719]

Gatenby PA, Ramus JR, Caygill CP, Shepherd NA, Watson A. Relevance of the detection of intestinal metaplasia in non-dysplastic columnar-lined oesophagus. Scand J Gastroenterol. 2008; 43:524–530. [PubMed: 18415743]

Giannakis M, Stappenbeck TS, Mills JC, Leip DG, Lovett M, Clifton SW, Ippolito JE, Glasscock JI, Arumugam M, Brent MR, Gordon JI. Molecular properties of adult mouse gastric and intestinal epithelial progenitors in their niches. J Biol Chem. 2006; 281:11292–11300. [PubMed: 16464855]

Goldblum JR. Controversies in the Diagnosis of Barrett Esophagus and Barrett-Related Dysplasia: One Pathologist's Perspective. Arch Pathol Lab Med. 2010; 134:1479–1484. [PubMed: 20923304]

Gough MD, Ackroyd R, Majeed AW, Bird NC. Prediction of malignant potential in reflux disease: are cytokine polymorphisms important? Am J Gastroenterol. 2005; 100:1012–1018. [PubMed: 15842572]

Grivennikov S, Karin M. Autocrine IL-6 signaling: a key event in tumorigenesis? Cancer Cell. 2008; 13:7–9. [PubMed: 18167335]

Grivennikov SI, Greten FR, Karin M. Immunity, inflammation, and cancer. Cell. 2010; 140:883–899. [PubMed: 20303878]

Hamilton SR, Yardley JH. Regnerative of cardiac type mucosa and acquisition of Barrett mucosa after esophagogastrostomy. Gastroenterology. 1977; 72:669–675. [PubMed: 838221]

Hanby AM, Jankowski JA, Elia G, Poulsom R, Wright NA. Expression of the trefoil peptides pS2 and human spasmolytic polypeptide (hSP) in Barrett's metaplasia and the native oesophageal epithelium: delineation of epithelial phenotype. J Pathol. 1994; 173:213–219. [PubMed: 7931841]

Howlett M, Giraud AS, Lescesen H, Jackson CB, Kalantzis A, Van Driel IR, Robb L, Van der Hoek M, Ernst M, Minamoto T, et al. The interleukin-6 family cytokine interleukin-11 regulates homeostatic epithelial cell turnover and promotes gastric tumor development. Gastroenterology. 2009; 136:967–977. [PubMed: 19121317]

Hvid-Jensen F, Pedersen L, Drewes AM, Sorensen HT, Funch-Jensen P. Incidence of adenocarcinoma among patients with Barrett's esophagus. The New England journal of medicine. 2011; 365:1375–1383. [PubMed: 21995385]

NIH-PA Author Manuscript

NIH-PA Author Manuscript

NIH-PA Author Manuscript

Jankowski JA, Harrison RF, Perry I, Balkwill F, Tselepis C. Barrett's metaplasia. Lancet. 2000; 356:2079–2085. [PubMed: 11145505]

Jankowski JA, Wright NA, Meltzer SJ, Triadafilopoulos G, Geboes K, Casson AG, Kerr D, Young LS. Molecular evolution of the metaplasia-dysplasia-adenocarcinoma sequence in the esophagus. Am J Pathol. 1999; 154:965–973. [PubMed: 10233832]

Jiang L, Gonda TA, Gamble MV, Salas M, Seshan V, Tu S, Twaddell WS, Hegyi P, Lazar G, Steele I, et al. Global hypomethylation of genomic DNA in cancer-associated myofibroblasts. Cancer Res. 2008; 68:9900–9908. [PubMed: 19047171]

Jin G, Ramanathan V, Quante M, Baik GH, Yang X, Wang SS, Tu S, Gordon SA, Pritchard DM, Varro A, et al. Inactivating cholecystokinin-2 receptor inhibits progastrin-dependent colonic crypt fission, proliferation, and colorectal cancer in mice. J Clin Invest. 2009; 119:2691–2701. [PubMed: 19652364]

Kalabis J, Oyama K, Okawa T, Nakagawa H, Michaylira CZ, Stairs DB, Figueiredo JL, Mahmood U, Diehl JA, Herlyn M, Rustgi AK. A subpopulation of mouse esophageal basal cells has properties of stem cells with the capacity for self-renewal and lineage specification. J Clin Invest. 2008; 118:3860–3869. [PubMed: 19033657]

Kauer WK, Peters JH, DeMeester TR, Feussner H, Ireland AP, Stein HJ, Siewert RJ. Composition and concentration of bile acid reflux into the esophagus of patients with gastroesophageal reflux disease. Surgery. 1997; 122:874–881. [PubMed: 9369886]

Kazumori H, Ishihara S, Rumi MA, Kadowaki Y, Kinoshita Y. Bile acids directly augment caudal related homeobox gene Cdx2 expression in oesophageal keratinocytes in Barrett's epithelium. Gut. 2006; 55:16–25. [PubMed: 16118348]

Kelty CJ, Gough MD, Van Wyk Q, Stephenson TJ, Ackroyd R. Barrett's oesophagus: intestinal metaplasia is not essential for cancer risk. Scand J Gastroenterol. 2007; 42:1271–1274. [PubMed: 17852872]

Kim TH, Shivdasani RA. Notch signaling in stomach epithelial stem cell homeostasis. J Exp Med. 2011

Leedham SJ, Preston SL, McDonald SA, Elia G, Bhandari P, Poller D, Harrison R, Novelli MR, Jankowski JA, Wright NA. Individual crypt genetic heterogeneity and the origin of metaplastic glandular epithelium in human Barrett's oesophagus. Gut. 2008; 57:1041–1048. [PubMed: 18305067]

Means AL, Xu Y, Zhao A, Ray KC, Gu G. A CK19(CreERT) knockin mouse line allows for conditional DNA recombination in epithelial cells in multiple endodermal organs. Genesis. 2008; 46:318–323. [PubMed: 18543299]

Menke V, van Es JH, de Lau W, van den Born M, Kuipers EJ, Siersema PD, de Bruin RW, Kusters JG, Clevers H. Conversion of metaplastic Barrett's epithelium into post-mitotic goblet cells by gamma-secretase inhibition. Dis Model Mech. 2010; 3:104–110. [PubMed: 20075383]

Milano F, van Baal JW, Buttar NS, Rygiel AM, de Kort F, DeMars CJ, Rosmolen WD, Bergman JJ, JVAM, Wang KK, et al. Bone morphogenetic protein 4 expressed in esophagitis induces a columnar phenotype in esophageal squamous cells. Gastroenterology. 2007; 132:2412–2421. [PubMed: 17570215]

Nakagawa H, Wang TC, Zukerberg L, Odze R, Togawa K, May GH, Wilson J, Rustgi AK. The targeting of the cyclin D1 oncogene by an Epstein-Barr virus promoter in transgenic mice causes dysplasia in the tongue, esophagus and forestomach. Oncogene. 1997; 14:1185–1190. [PubMed: 9121767]

Nakanishi Y, Saka M, Eguchi T, Sekine S, Taniguchi H, Shimoda T. Distribution and significance of the oesophageal and gastric cardiac mucosae: a study of 131 operation specimens. Histopathology. 2007; 51:515–519. [PubMed: 17711448]

O'Riordan JM, Abdel-latif MM, Ravi N, McNamara D, Byrne PJ, McDonald GS, Keeling PW, Kelleher D, Reynolds JV. Proinflammatory cytokine and nuclear factor kappa-B expression along the inflammation-metaplasia-dysplasia-adenocarcinoma sequence in the esophagus. Am J Gastroenterol. 2005; 100:1257–1264. [PubMed: 15929754]

Odze RD, Maley CC. Neoplasia without dysplasia: lessons from Barrett esophagus and other tubal gut neoplasms. Arch Pathol Lab Med. 2010; 134:896–906. [PubMed: 20524867]

NIH-PA Author Manuscript

NIH-PA Author Manuscript

NIH-PA Author Manuscript

Ogiya K, Kawano T, Ito E, Nakajima Y, Kawada K, Nishikage T, Nagai K. Lower esophageal palisade vessels and the definition of Barrett's esophagus. Dis Esophagus. 2008; 21:645–649. [PubMed: 18459993]

Payne CM, Crowley-Weber CL, Dvorak K, Bernstein C, Bernstein H, Holubec H, Crowley C, Garewal H. Mitochondrial perturbation attenuates bile acid-induced cytotoxicity. Cell Biol Toxicol. 2005; 21:215–231. [PubMed: 16323058]

Pera M, de Bolos C, Brito MJ, Palacin A, Grande L, Cardesa A, Poulsom R. Duodenal-content reflux into the esophagus leads to expression of Cdx2 and Muc2 in areas of squamous epithelium in rats. J Gastrointest Surg. 2007; 11:869–874. [PubMed: 17440788]

Playford RJ. New British Society of Gastroenterology (BSG) guidelines for the diagnosis and management of Barrett's oesophagus. Gut. 2006; 55:442. [PubMed: 16531521]

Quante M, Marrache F, Goldenring JR, Wang TC. TFF2 mRNA transcript expression marks a gland progenitor cell of the gastric oxyntic mucosa. Gastroenterology. 2010

Riddell RH, Odze RD. Definition of Barrett's esophagus: time for a rethink--is intestinal metaplasia dead? Am J Gastroenterol. 2009; 104:2588–2594. [PubMed: 19623166]

Sarosi G, Brown G, Jaiswal K, Feagins LA, Lee E, Crook TW, Souza RF, Zou YS, Shay JW, Spechler SJ. Bone marrow progenitor cells contribute to esophageal regeneration and metaplasia in a rat model of Barrett's esophagus. Dis Esophagus. 2008; 21:43–50. [PubMed: 18197938]

Sato F, Meltzer SJ. CpG island hypermethylation in progression of esophageal and gastric cancer. Cancer. 2006; 106:483–493. [PubMed: 16362978]

Shaheen NJ, Sharma P, Overholt BF, Wolfsen HC, Sampliner RE, Wang KK, Galanko JA, Bronner MP, Goldblum JR, Bennett AE, et al. Radiofrequency ablation in Barrett's esophagus with dysplasia. The New England journal of medicine. 2009; 360:2277–2288. [PubMed: 19474425]

Spechler SJ, Fitzgerald RC, Prasad GA, Wang KK. History, molecular mechanisms, and endoscopic treatment of Barrett's esophagus. Gastroenterology. 2010; 138:854–869. [PubMed: 20080098]

Stairs DB, Bayne LJ, Rhoades B, Vega ME, Waldron TJ, Kalabis J, Klein-Szanto A, Lee JS, Katz JP, Diehl JA, et al. Deletion of p120-Catenin Results in a Tumor Microenvironment with Inflammation and Cancer that Establishes It as a Tumor Suppressor Gene. Cancer Cell. 2011; 19:470–483. [PubMed: 21481789]

Stairs DB, Nakagawa H, Klein-Szanto A, Mitchell SD, Silberg DG, Tobias JW, Lynch JP, Rustgi AK. Cdx1 and c-Myc foster the initiation of transdifferentiation of the normal esophageal squamous epithelium toward Barrett's esophagus. PLoS One. 2008; 3:e3534. [PubMed: 18953412]

Takubo K, Aida J, Naomoto Y, Sawabe M, Arai T, Shiraishi H, Matsuura M, Ell C, May A, Pech O, et al. Cardiac rather than intestinal-type background in endoscopic resection specimens of minute Barrett adenocarcinoma. Hum Pathol. 2009; 40:65–74. [PubMed: 18755496]

Tatsuta T, Mukaisho K, Sugihara H, Miwa K, Tani T, Hattori T. Expression of Cdx2 in early GRCL of Barrett's esophagus induced in rats by duodenal reflux. Dig Dis Sci. 2005; 50:425–431. [PubMed: 15810620]

Theisen J, Nehra D, Citron D, Johansson J, Hagen JA, Crookes PF, DeMeester SR, Bremner CG, DeMeester TR, Peters JH. Suppression of gastric acid secretion in patients with gastroesophageal reflux disease results in gastric bacterial overgrowth and deconjugation of bile acids. J Gastrointest Surg. 2000; 4:50–54. [PubMed: 10631362]

Tomita H, Takaishi S, Menheniott TR, Yang X, Shibata W, Jin G, Betz KS, Kawakami K, Minamoto T, Tomasetto C, et al. Inhibition of gastric carcinogenesis by the hormone gastrin is mediated by suppression of TFF1 epigenetic silencing. Gastroenterology. 2010 (in press).

Tu S, Bhagat G, Cui G, Takaishi S, Kurt-Jones EA, Rickman B, Betz KS, Penz-Oesterreicher M, Bjorkdahl O, Fox JG, Wang TC. Overexpression of interleukin-1beta induces gastric inflammation and cancer and mobilizes myeloid-derived suppressor cells in mice. Cancer Cell. 2008; 14:408–419. [PubMed: 18977329]

Vaccaro BJ, Gonzalez S, Poneros JM, Stevens PD, Capiak KM, Lightdale CJ, Abrams JA. Detection of intestinal metaplasia after successful eradication of Barrett's Esophagus with radiofrequency ablation. Dig Dis Sci. 2011; 56:1996–2000. [PubMed: 21468652]

NIH-PA Author Manuscript

NIH-PA Author Manuscript

NIH-PA Author Manuscript

Van De Bovenkamp JH, Korteland-Van Male AM, Warson C, Buller HA, Einerhand AW, Ectors NL, Dekker J. Gastric-type mucin and TFF-peptide expression in Barrett's oesophagus is disturbed during increased expression of MUC2. Histopathology. 2003; 42:555–565. [PubMed: 12786891]

Wang DH, Clemons NJ, Miyashita T, Dupuy AJ, Zhang W, Szczepny A, Corcoran-Schwartz IM, Wilburn DL, Montgomery EA, Wang JS, et al. Aberrant epithelial-mesenchymal Hedgehog signaling characterizes Barrett's metaplasia. Gastroenterology. 138:1810–1822. [PubMed: 20138038]

Wang X, Ouyang H, Yamamoto Y, Kumar PA, Wei TS, Dagher R, Vincent M, Lu X, Bellizzi AM, Ho KY, et al. Residual embryonic cells as precursors of a Barrett's-like metaplasia. Cell. 2011; 145:1023–1035. [PubMed: 21703447]

Warson C, Van De Bovenkamp JH, Korteland-Van Male AM, Buller HA, Einerhand AW, Ectors NL, Dekker J. Barrett's esophagus is characterized by expression of gastric-type mucins (MUC5AC, MUC6) and TFF peptides (TFF1 and TFF2), but the risk of carcinoma development may be indicated by the intestinal-type mucin, MUC2. Hum Pathol. 2002; 33:660–668. [PubMed: 12152167]

Watanabe F, Iwasaki Y, Ohashi M, Nunobe S, Iwagami S, Takahashi K, Yamaguchi T, Matsumoto H, Yasutome M. A case report-the marked response to S-1 + CDDP chemotherapy for post-operative local recurrence of advanced gastric cancer. Gan To Kagaku Ryoho. 2007; 34:1970–1972. [PubMed: 18219868]

Winter JW, Paterson S, Scobie G, Wirz A, Preston T, McColl KE. N-nitrosamine generation from ingested nitrate via nitric oxide in subjects with and without gastroesophageal reflux. Gastroenterology. 2007; 133:164–174. [PubMed: 17631140]

Yang XD, Ai W, Asfaha S, Bhagat G, Friedman RA, Jin G, Park H, Shykind B, Diacovo TG, Falus A, Wang TC. Histamine deficiency promotes inflammation-associated carcinogenesis through reduced myeloid maturation and accumulation of CD11b+Ly6G+ immature myeloid cells. Nature Medicine. 2010

Yu WY, Slack JM, Tosh D. Conversion of columnar to stratified squamous epithelium in the developing mouse oesophagus. Dev Biol. 2005; 284:157–170. [PubMed: 15992795]

NIH-PA Author Manuscript

NIH-PA Author Manuscript

NIH-PA Author Manuscript

Significance

Using a transgenic mouse model of BE and EAC, that closely resembles the human disease, insights into the pathogenesis of BE are provided. A gastric cardia progenitor cell lineage appears to be activated by bile acid induced and IL-1β and IL-6 dependent inflammation, inducing migration into the distal esophagus where it gives rise to columnar-like metaplasia and dysplasia. Activated Notch signaling appears to regulates differentiation of the cardia progenitor into intestinal-type columnar cells instead of goblet cells, and is associated with a malignant transformation in mice and humans. Our findings challenge the common paradigms regarding the pathogenesis BE and EAC.

NIH-PA Author Manuscript

NIH-PA Author Manuscript

NIH-PA Author Manuscript

Highlights

- IL-1β overexpression in the mouse esophagus induces IL-6 dependent BE and EAC.
- Bile acids accelerate intestinal metaplasia and dysplasia in this mouse model of BE.
- Notch signaling in columnar cells, not goblet cells is associated with carcinogenesis
- BE and EAC likely arise from gastric cardia progenitor cells

NIH-PA Author Manuscript
NIH-PA Author Manuscript
NIH-PA Author Manuscript

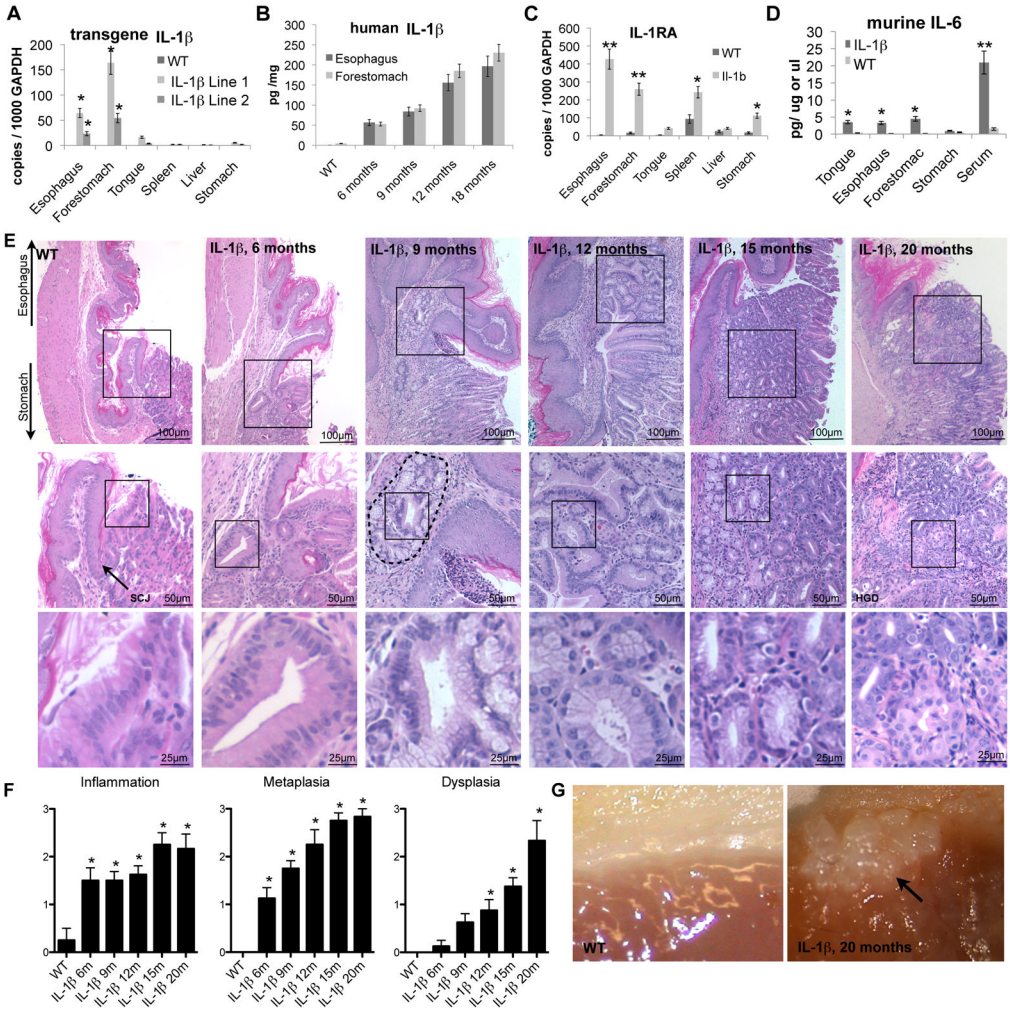

Figure 1. Overexpression of IL-1β induced chronic inflammation in the murine esophagus and step-wise development of metaplasia and dysplasia at the SCJ

(A) mRNA expression (RT-qPCR) in different organs of 3 month old two founder *L2-IL-1β*-lines.

(B) ELISA for human (transgenic) IL-1β showed age dependent hIL-1β protein expression levels.

(C) mRNA expression (RT-qPCR) of IL1-receptor-antagonist (*IL1ra*) in different organs in 12 months old *L2-IL-1β* mice compared to WT littermates.

(D) ELISA for serum levels and organ protein expression of mIL-6 in *L2-IL-1β* mice compared to WT (C57/B6) littermates.

(E) Histopathologic changes in *L2-IL-1β* mice occurred at the squamo-columnar junction (SCJ, arrow in WT). Representative pictures of WT and 6, 9, 12, 15, and 20 months old *L2-IL-1β*, top panels show an overview of the SCJ, where the squamous esophagus epithelium meets the columnar cardia/stomach epithelium, second and third panels show insert magnifications of the stepwise progression to BE and EAC.

(F) Histopathologic scoring of 6, 9, 12, 15, and 20 months old *L2-IL-1β* mice compared to WT (C57/B6) littermates.

(G) Representative gross pictures of the SCJ in WT and 20 months old *L2-IL-1β* mice with tumor (arrow).

(data are represented as mean +/−SEM *p<0.05, **p<0.01) See also Figure S1.

NIH-PA Author Manuscript

NIH-PA Author Manuscript

NIH-PA Author Manuscript

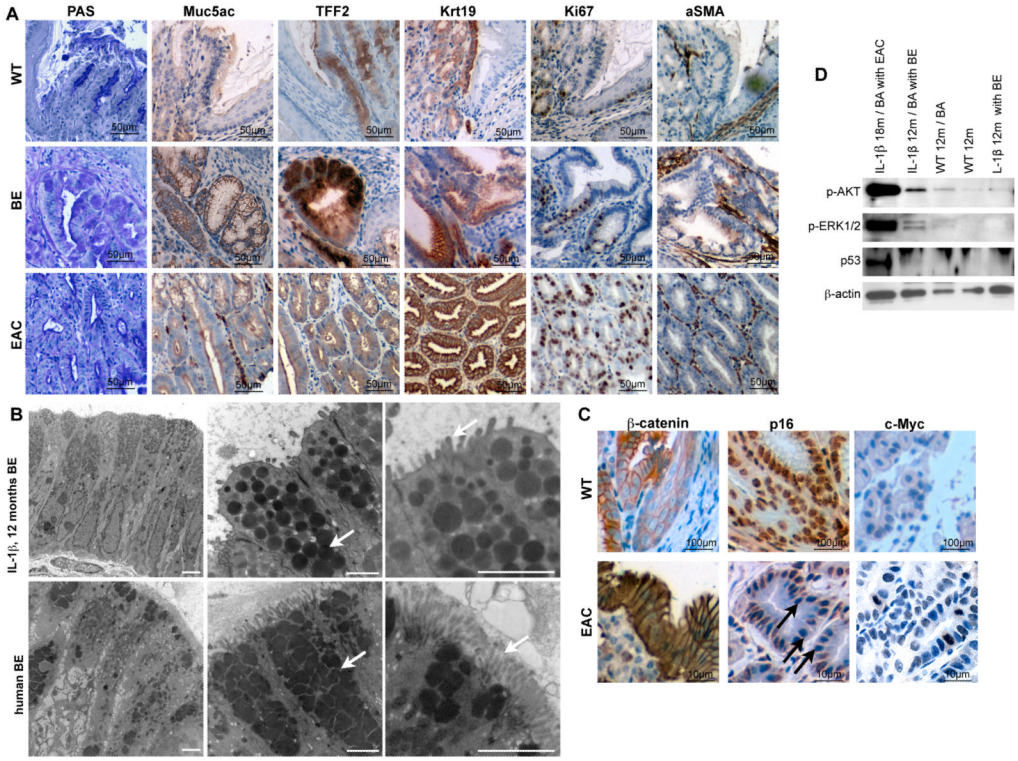

Figure 2. The IL-1β mouse model resembles the human disease

(A) Representative pictures of staining for PAS, Muc5ac, Krt19, Tff2, Ki67, and aSma of normal SCJ histology in WT (left panel), BE histology in 15 months old *L2-IL-1β* mice (middle panel), and HGD histology in 22 months old *L2-IL-1β* mice (right panel).

(B) Representative electron microscopy pictures of mouse (top panel) human (bottom panel) BE epithelium showing columnar cells (left), granules with mucin (middle), and microvilli (right) (scale bar: 2μm).

(C) Representative pictures of β-catenin, p16 and c-myc in WT mice and dysplastic tissue of 16 months old BA-treated *L2-IL-1β* mice.

(D) Western Blot for p53, p-Erk and p-Akt in indicated tissues, showing p53 stabilization, and activation of Akt and Erk pathways in EAC and BA treated BE. See also Figure S2 and Table S1.

NIH-PA Author Manuscript

NIH-PA Author Manuscript

NIH-PA Author Manuscript

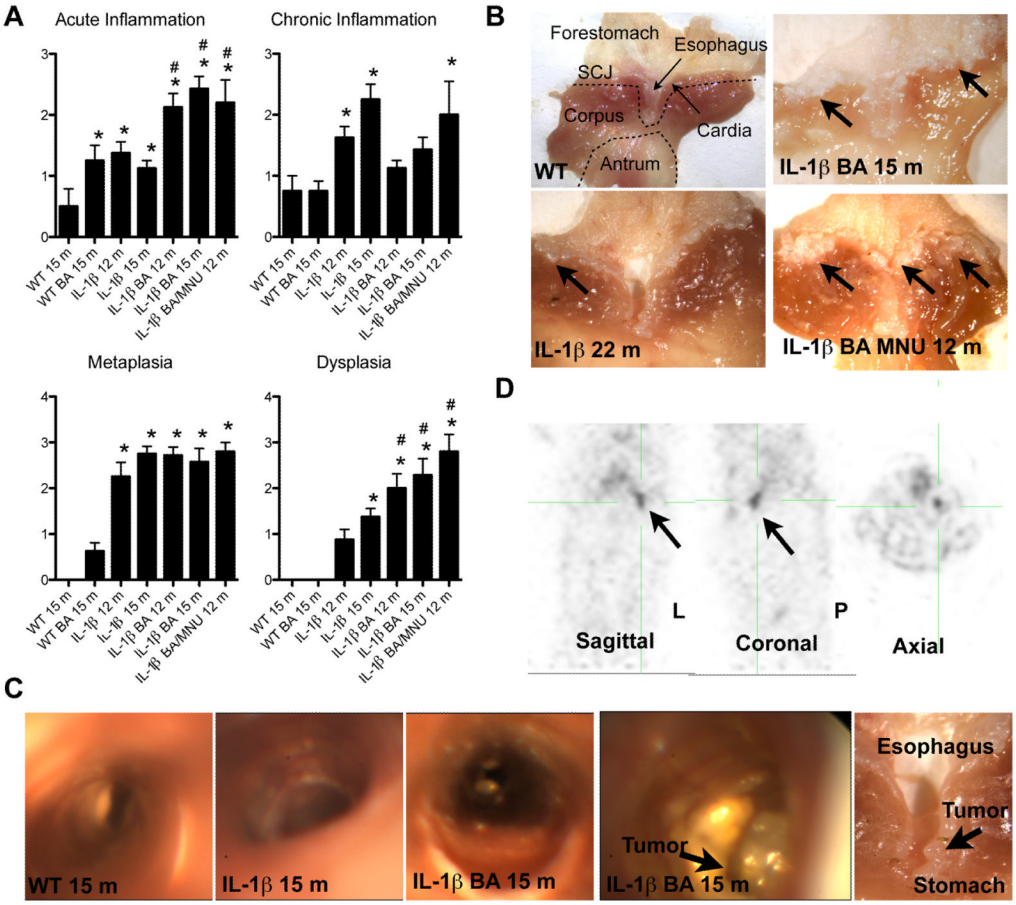

Figure 3. Bile acids and carcinogens accelerate the development of Barrett's metaplasia and dysplasia

(A) Histopathological scoring of 6, 9, 12, and 15, months old BA-treated *L2-IL-1β* mice and combined 12 months old BA and N-Methyl-N-nitrosourea (MNU)-treated *L2-IL-1β* mice compared to WT (C57/B6) littermates (*p<0.05 compared to WT, #p<0.05 compared to untreated *L2-IL-1β* mice).

(B) Representative gross pictures of the SCJ in WT, 22 months old *L2-IL-1β* mice 15 months old BA-treated *L2-IL-1β* mice and combined BA and MNU-treated 12-month-old *L2-IL-1β* mice with tumors at the SCJ.

(C) Representative pictures of the esophagus and SCJ during upper endoscopy in intact 15-month-old BA treated or untreated *L2-IL-1β* mice Ant WT mice and corresponding gross macroscopic evaluation (right).

(D) PET imaging was performed on a rodent microPET scanner to measure glucose uptake in tumors relative to normal tissue. A representative picture of 15-month-old BA treated *L2-IL-1β* mice is shown in sagittal, coronal and axial position (arrow indicates the tumor, that was macroscopically and histologically confirmed) See also Movie S1-5. (data are represented as mean +/−SEM) See also Figure S3.

NIH-PA Author Manuscript

NIH-PA Author Manuscript

NIH-PA Author Manuscript

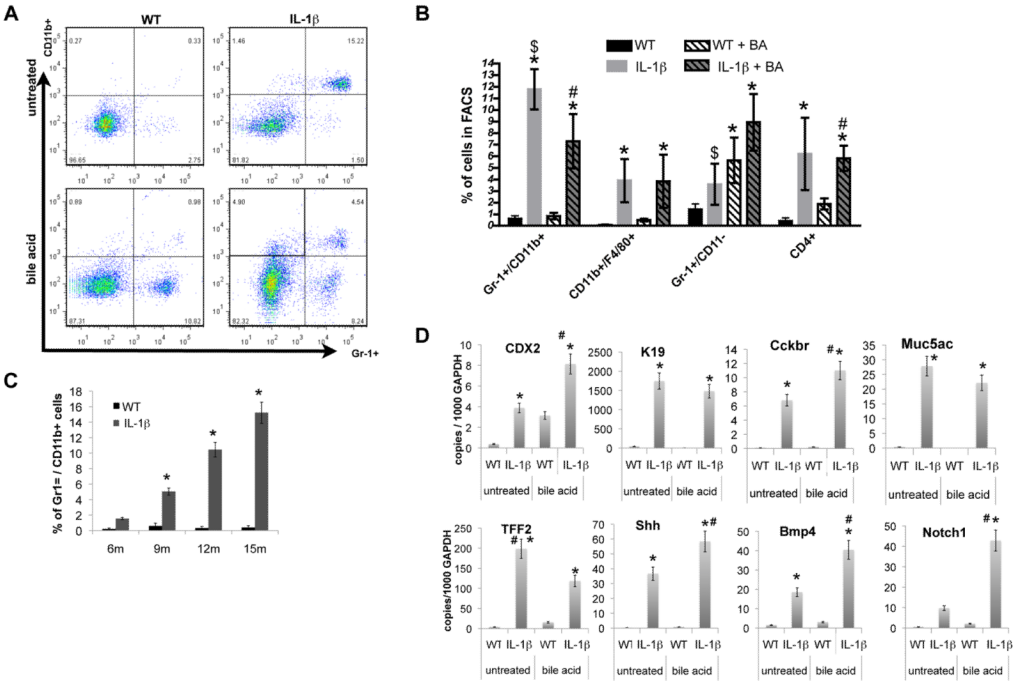

Figure 4. Bile acids induce an acute and chronic immune response and activate Notch signaling in BE

(A) The frequencies of lymphoid and myeloid cells in the esophagus from 12-month-old *L2-IL-1β* mice and age-matched WT mice were measured by FACS, and representative FACS blots for detecting immature (CD11b+Gr1+) myeloid cells in the esophagus from WT, *L2-IL-1β* mice, BA-treated WT, and BA-treated *L2-IL-1β* mice are shown.

(B) Quantitative analysis of FACS for immature (CD11b+Gr1+) myeloid cells, neutrophiles/granulocytes (CD11b-Gr1+), macrophages (Cd11b+/F4/80+), and T-cells (CD4+) (*p<0.05 compared to WT, #p<0.05 compared to BA treated WT, $p<0.05 compared to untreated *L2-IL-1β* mice).

(C) Quantitative analysis of FACS for immature (CD11b+Gr1+) myeloid cells in 6, 9, 12, 15 month-old *L2-IL-1β* mice compared to age-matched WT mice.

(D) mRNA expression (RT-qPCR) of Cdx2, K19, Cckbr, Muc5ac, TFF2, Shh, Bmp4, and Notch1 in the SCJ tissue of WT, *L2-IL-1β* mice, BA-treated WT, and BA-treated *L2-IL-1β* mice (*p<0.01 compared to WT, # p<0.05 compared to *L2-IL-1β* mice).

NIH-PA Author Manuscript
NIH-PA Author Manuscript
NIH-PA Author Manuscript

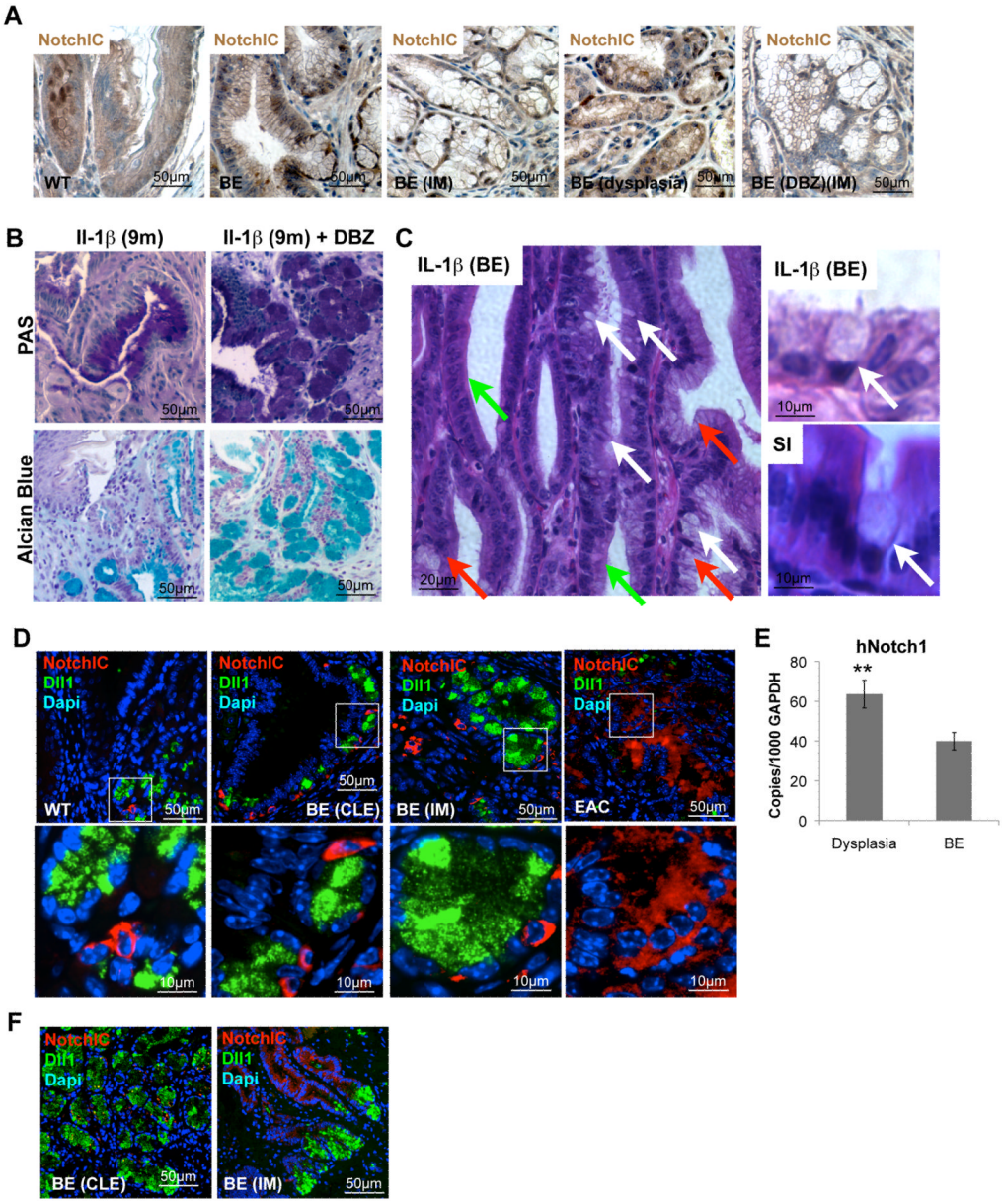

Figure 5. Notch signaling in BE

(A) Representative pictures of NotchIC IHC in 15 month-old *L2-IL-1β* BA treated mice and 9 month-old *L2-IL-1β* mice after γ-secretase inhibitor treatment (DBZ).

(B) Representative pictures of periodic acid-Schiff (PAS) and Alcain-Blue staining at the SCJ of 9 months old *L2-IL*-1β without and with 10 days γ-secretase inhibitor treatment (right, Notch signaling inhibitor, DBZ).

(C) Representative picture of BE in γ-secretase treated *L2-IL-1β* mice showing occasional true goblet cells (White arrows), CLE (green arrows) and goblet like cells (red arrows) on the left. On the right goblet cells in BE (top) and small intestine (SI, bottom) are shown to show similarities in intestinal metaplasia.

(D) Representative pictures of NotchIC (red) and Delta-Like1 (DII1) (green) IHC in 9 month old WT, 9 months old *L2-IL*-1β with BE, and 15 months old BA treated *L2-IL*-1β with EAC, inserts label magnified area below

NIH-PA Author Manuscript

NIH-PA Author Manuscript

NIH-PA Author Manuscript

(E) mRNA expression (RT-qPCR) of *Notch1* in biopsies of esophageal tissue, obtained from 46 patients with BE with and without dysplasia. In each patient, biopsies were taken from Barrett's mucosa and from dysplastic appearing mucosa
(F) Representative pictures of NotchIC (red) and Delta-Like1 (DII1) (green) IHC in human BE with CLE or IM. See also Figure S4, and Table S2. (data are represented as mean +/−SEM *$p<0.05$)

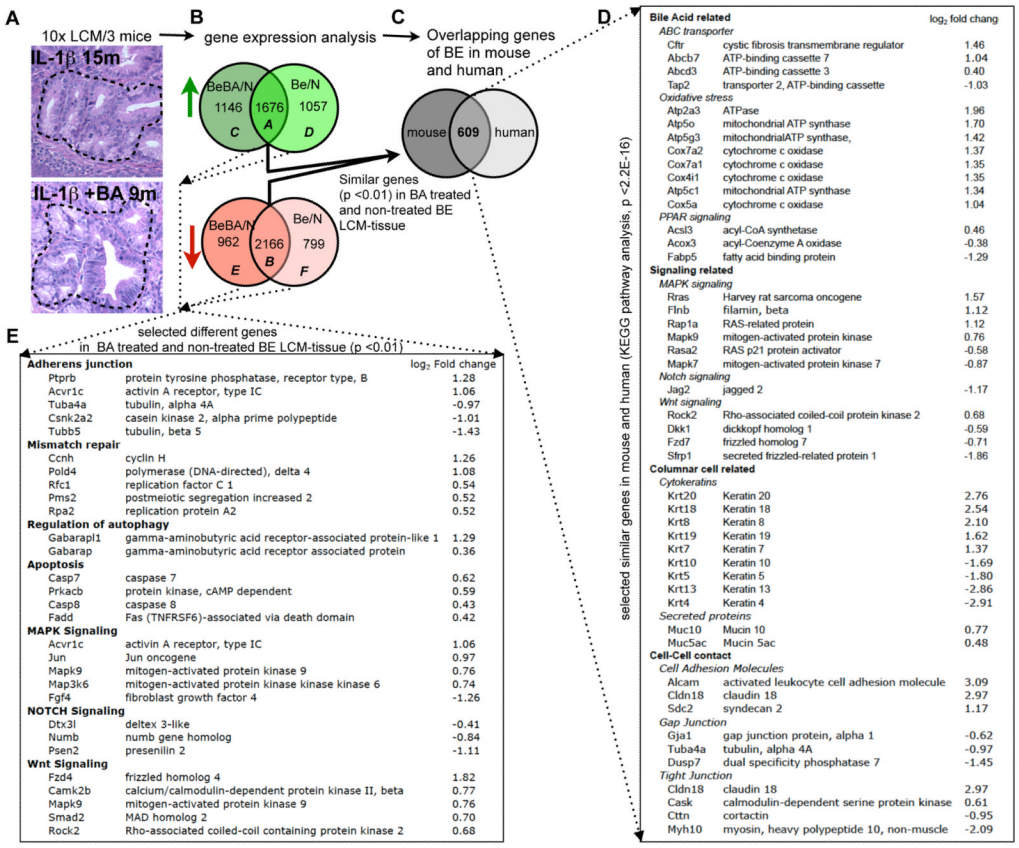

Adherens junction		log2 Fold change
Ptprb	protein tyrosine phosphatase, receptor type, B	1.28
Acvr1c	activin A receptor, type IC	1.06
Tuba4a	tubulin, alpha 4A	-0.97
Csnk2a2	casein kinase 2, alpha prime polypeptide	-1.01
Tubb5	tubulin, beta 5	-1.43
Mismatch repair		
Ccnh	cyclin H	1.26
Pold4	polymerase (DNA-directed), delta 4	1.08
Rfc1	replication factor C 1	0.54
Pms2	postmeiotic segregation increased 2	0.52
Rpa2	replication protein A2	0.52
Regulation of autophagy		
Gabarapl1	gamma-aminobutyric acid receptor-associated protein-like 1	1.29
Gabarap	gamma-aminobutyric acid receptor associated protein	0.36
Apoptosis		
Casp7	caspase 7	0.62
Prkacb	protein kinase, cAMP dependent	0.59
Casp8	caspase 8	0.43
Fadd	Fas (TNFRSF6)-associated via death domain	0.42
MAPK Signaling		
Acvr1c	activin A receptor, type IC	1.06
Jun	Jun oncogene	0.97
Mapk9	mitogen-activated protein kinase 9	0.76
Map3k6	mitogen-activated protein kinase kinase kinase 6	0.74
Fgf4	fibroblast growth factor 4	-1.26
NOTCH Signaling		
Dtx3l	deltex 3-like	-0.41
Numb	numb gene homolog	-0.84
Psen2	presenilin 2	-1.11
Wnt Signaling		
Fzd4	frizzled homolog 4	1.82
Camk2b	calcium/calmodulin-dependent protein kinase II, beta	0.77
Mapk9	mitogen-activated protein kinase 9	0.76
Smad2	MAD homolog 2	0.70
Rock2	Rho-associated coiled-coil containing protein kinase 2	0.68

Bile Acid related		log2 fold chang
ABC transporter		
Cftr	cystic fibrosis transmembrane regulator	1.46
Abcb7	ATP-binding cassette 7	1.04
Abcd3	ATP-binding cassette 3	0.40
Tap2	transporter 2, ATP-binding cassette	-1.03
Oxidative stress		
Atp2a3	ATPase	1.96
Atp5o	mitochondrial ATP synthase	1.70
Atp5g3	mitochondrialATP synthase,	1.42
Cox7a2	cytochrome c oxidase	1.37
Cox7a1	cytochrome c oxidase	1.35
Cox4i1	cytochrome c oxidase	1.35
Atp5c1	mitochondrial ATP synthase	1.34
Cox5a	cytochrome c oxidase	1.04
PPAR signaling		
Acsl3	acyl-CoA synthetase	0.46
Acox3	acyl-Coenzyme A oxidase	-0.38
Fabp5	fatty acid binding protein	-1.29
Signaling related		
MAPK signaling		
Rras	Harvey rat sarcoma oncogene	1.57
Flnb	filamin, beta	1.12
Rap1a	RAS-related protein	1.12
Mapk9	mitogen-activated protein kinase	0.76
Rasa2	RAS p21 protein activator	-0.58
Mapk7	mitogen-activated protein kinase 7	-0.87
Notch signaling		
Jag2	jagged 2	-1.17
Wnt signaling		
Rock2	Rho-associated coiled-coil protein kinase 2	0.68
Dkk1	dickkopf homolog 1	-0.59
Fzd7	frizzled homolog 7	-0.71
Sfrp1	secreted frizzled-related protein 1	-1.86
Columnar cell related		
Cytokeratins		
Krt20	Keratin 20	2.76
Krt18	Keratin 18	2.54
Krt8	Keratin 8	2.10
Krt19	Keratin 19	1.62
Krt7	Keratin 7	1.37
Krt10	Keratin 10	-1.69
Krt5	Keratin 5	-1.80
Krt13	Keratin 13	-2.86
Krt4	Keratin 4	-2.91
Secreted proteins		
Muc10	Mucin 10	0.77
Muc5ac	Mucin 5ac	0.48
Cell-Cell contact		
Cell Adhesion Molecules		
Alcam	activated leukocyte cell adhesion molecule	3.09
Cldn18	claudin 18	2.97
Sdc2	syndecan 2	1.17
Gap Junction		
Gja1	gap junction protein, alpha 1	-0.62
Tuba4a	tubulin, alpha 4A	-0.97
Dusp7	dual specificity phosphatase 7	-1.45
Tight Junction		
Cldn18	claudin 18	2.97
Cask	calmodulin-dependent serine protein kinase	0.61
Cttn	cortactin	-0.95
Myh10	myosin, heavy polypeptide 10, non-muscle	-2.09

Figure 6. Gene expression profiles of mouse BE resembles that of the human disease

(A) Laser capture microdissection (LCM) was applied to typical metaplastic lesions at the SCJ in 15 month-old *L2-IL-1β* mice or 9 months old BA-treated *L2-IL-1β* mice and to the squamous epithelium of WT control mice. A schematic sequence of the experimental procedures is shown: (A) After LCM (a representative outlined area is shown) followed by RNA isolation and amplification, (B) Venn diagram mouse BE *vs* BA-treated mouse BE: Gene expression of BE tissue from untreated *L2-IL-1β* mice (n=3, BE *vs* N) and BA-treated *L2-IL-1β* mice (n=3, BeBA *vs* N) was compared to WT squamous tissue (n=3) in order to determine the overlapping up- and down-regulated genes in both cohorts.

(C) Venn diagram mouse *vs* human: These 3832 significantly different genes (1676 up (Venn diagram: A) and 2166 down (Venn diagram: B), $p<0.01$) were than compared to the gene expression pattern of a human expression analysis (Stairs et al., 2008) where human BE tissue was compared to human esophageal squamous tissue. This comparison identified 606 genes, which were analyzed by KEGG pathway analysis.

(D) A list of these significantly identical genes in human and mouse is shown with the $\log_2$ fold change of the comparison of BA-treated *L2-IL-1β* mice compared to the squamous epithelium of WT control mice.

(E) KEGG pathway analysis also identified genes that were altered differentially in BE epithelium of *L2-IL-1β* mice versus BA-treated *L2-IL-1β* mice (Venn diagram: C-F). A list of significantly different genes is shown.

NIH-PA Author Manuscript NIH-PA Author Manuscript NIH-PA Author Manuscript

NIH-PA Author Manuscript

NIH-PA Author Manuscript

NIH-PA Author Manuscript

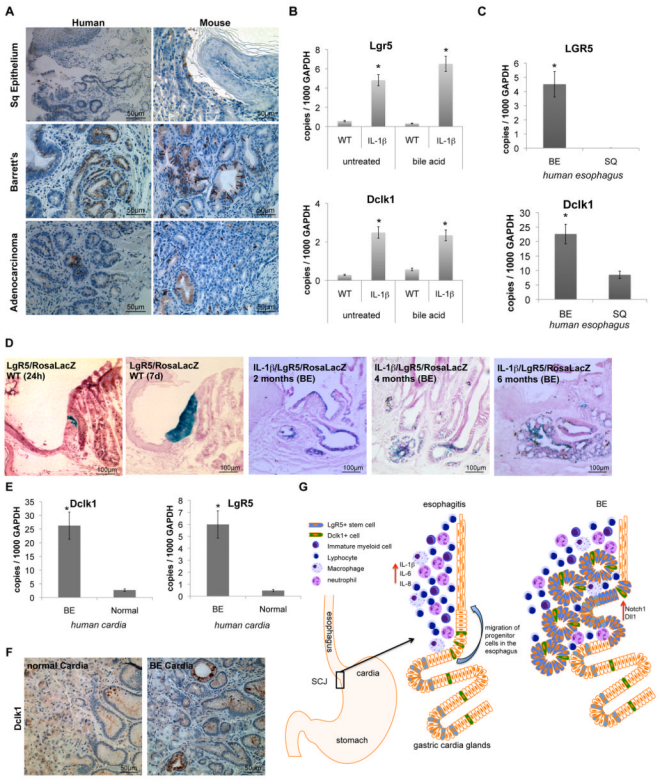

Figure 7. Barrett's metaplasia and dysplasia arise from gastric cardia progenitor cells in mice and humans

(A) Representative pictures of human (left) and mouse (right) SCJ, BE, and EAC tissue with Doublecortin like kinase-1 (Dclk1) IHC.

(B) mRNA expression (RT-qPCR) of Lgr5 and Dclk1 in the SCJ tissue of WT, *L2-IL-1β* mice, BA-treated WT, and BA-treated *L2-IL-1β* mice.

(C) mRNA expression (RT-qPCR) of *Lgr5* and *Dclk1* in biopsies of esophageal tissue, obtained from 46 patients with BE. In each patient, biopsies were taken from Barrett's mucosa and from normal-appearing squamous mucosa.

(D) Left: Lgr5-Cre-ERT x Rosa26r-lacZ mice were treated with 3-OH Tamoxifen and sacrificed 1d or 7d post induction. Analysis at 1d showed a small collection of Xgal+ cells in the cardia at the squamocolumnar junction (SCJ), while analysis at 7d showed complete lineage tracing of these columnar cardia glands. Right: Lineage tracing of BE tissue in 6 months old LgR5-CreERT/IL-1b/Rosa26LacZ mice. Tamoxifen induction (6mg in one does) was performed prior to bile acid treatment at the age of 4 weeks. Mice were sacrificed at 2, 4 or 6 months after induction, indicating lineage tracing of developing BE suggesting that Lgr5 cells might migrate into the distal esophagus and give rise to BE.

(E) mRNA expression (RT-qPCR) of *LGR5* and *DCLK*1 in biopsies of cardia tissue, obtained from 5 patients with BE and 5 patients without BE (normal).

(F) Representative DCLK1 IHC pictures of normal human cardia (left) and of cardia from patients with BE (right) with Doublecortin like kinase-1.

(G) Model: In a our model of the pathogenesis od BE and EAC in mice, bile acid treatment and IL-1β induced inflammation lead to migration of gastric cardia progenitor cells into the distal esophagus, giving rise to BE and EAC in association with increased Dll1-dependent Notch signaling which induced columnar cell differentiation (data are represented as mean +/−SEM *p<0.05)

NIH-PA Author Manuscript

NIH-PA Author Manuscript

NIH-PA Author Manuscript

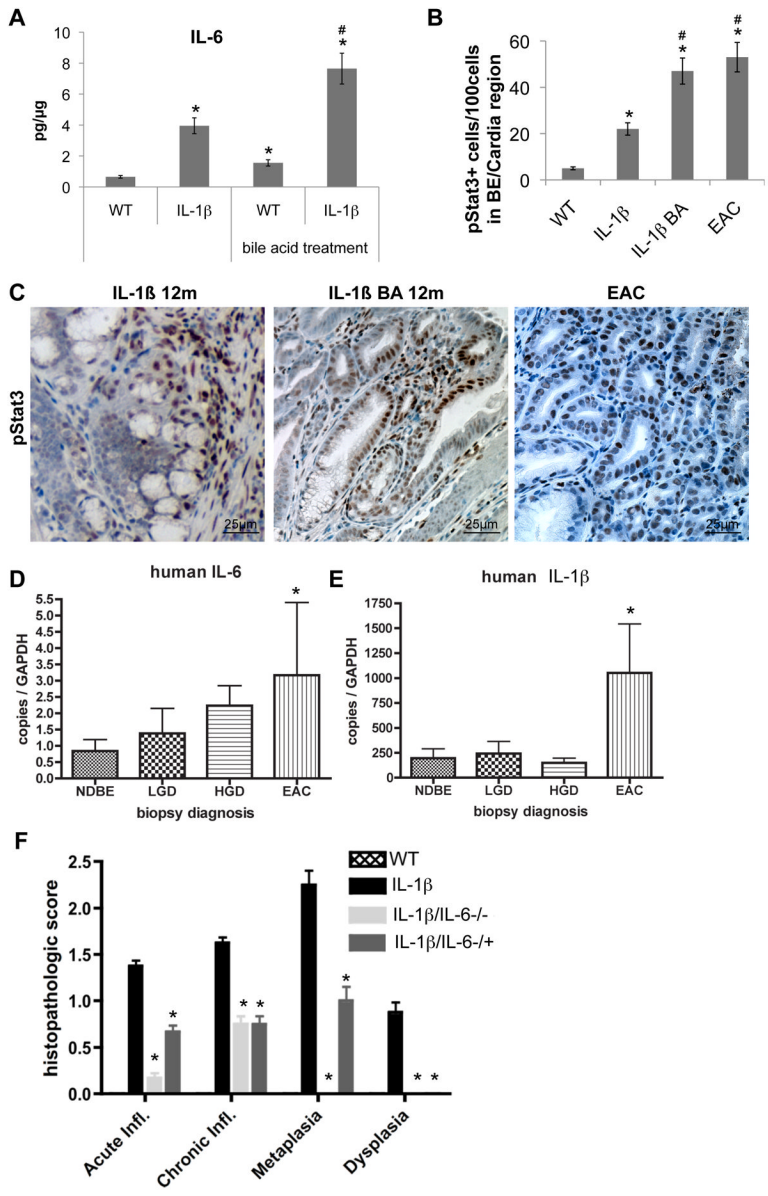

Figure 8. IL-6 deficiency abolishes IL-1β induced metaplasia and dysplasia

(A) mRNA expression (RT-qPCR) of IL-6 in the SCJ tissue of WT, *L2-IL-1β* mice, BA-treated WT, and BA-treated *L2-IL-1β* mice (*p<0.01 compared to WT, # p<0.05 compared to *L2-IL-1β* mice).

(B) Quantification of cells with phosphorilated STAT3 in WT, *L2-IL-1β* mice, BA-treated *L2-IL-1β*, and BA-treated *L2-IL-1β* mice with EAC (*p<0.01 compared to WT, # p<0.05 compared to *L2-IL-1β* mice)

(C) Representative pictures of pSTAT3 IHC in 12 month-old *L2-IL-1β* mice and BA-treated *L2-IL-1β*, and 15 month-old BA-treated *L2-IL-1β* mice with EAC.

(D and E) mRNA expression (RT-qPCR) of IL-6 (D) and IL-1β

(E) in biopsies of esophageal tissue, obtained from 46 patients with BE.

(F) Histopathological scoring of 12 month-old *L2-IL-1β* mice and *L2-IL-1β*/IL-6$^{-/-}$ or *L2-IL-1β*/IL-6$^{-/+}$ mice and WT (C57/B6) littermates (*p<0.05, compared to *L2-IL-1β* mice). See also Table S3 (data are represented as mean +/−SEM)